Jordanian Journal of Computers and Information Technology (JJCIT), Vol. 12, No. 02, June 2026.

FOUNTAIN CODES-BASED HYBRID SATELLITE TERRESTRIAL RELAY MULTICAST SCHEMES IN CO-CHANNEL INTERFERENCE ENVIRONMENT: OUTAGE PERFORMANCE, JOINT TIME AND POWER ALLOCATIONS

Nguyen Van Toan[1], Nguyen Ngoc Lan[2], Tran Trung Duy[2*], Pham Ngoc Son[3] and Nguyen Trung Hieu[2]

(Received: 1-Feb.-2026, Revised: 2-Apr.-2026 and 29-Apr-2026, Accepted: 29-Apr.-2026)

ABSTRACT

In this paper, we study outage performance of hybrid satellite-terrestrial relay multicast schemes employing Fountain codes. In the considered schemes, a satellite attempts to transmit its data to a group of ground users with the assistance of a terrestrial relay station. In the conventional scheme (referred to as ConV), the relay station forwards each Fountain packet to the ground users using decode-and-forward (DF). In the proposed scheme (referred to as ProP), the relay station stores Fountain packets received from the satellite and replaces the satellite in transmitting new Fountain packets to the ground users once it has collected a sufficient number of Fountain packets for data recovery. We derive exact closed-form expressions of outage probability (OP) at each user and system outage probability (SOP) for the ConV and ProP schemes, considering the impact of co-channel interference. Computer simulations are realized to validate the derived formulas. Moreover, a joint time and power allocation problem is formulated and solved to optimize the SOP performance for the two considered schemes.

KEYWORDS

Hybrid satellite-terrestrial relay multicast networks, Fountain codes, Co-channel interference, Outage probability, Joint time and power allocation.

1. INTRODUCTION

This work considers Hybrid Satellite-Terrestrial Relay (HSTR) schemes, in which terrestrial relays are utilized to facilitate communication between satellites and end users on the ground [1]-[3]. By integrating these relay stations, the HSTR schemes benefit from improved signal robustness, broader service areas, and greater reliability under challenging channel conditions. Such schemes are envisioned as a key enabler for next-generation infrastructures, offering high-speed access and minimal latency to meet future connectivity requirements. In [2], high-altitude platforms (HAPs) were presented as a complementary component to satellite networks within hybrid architectures, offering improved efficiency and addressing performance gaps in satellite-driven services, such as data relaying and fleet coordination. In [3], the authors proposed adaptive transmission schemes for HSTR networks to improve spectral and power efficiency in practical applications. Reference [4] introduced unmanned aerial vehicle (UAV)-aided maritime communication networks to enhance coverage and performance, acting as a supplementary layer to marine satellites and shore-based terrestrial stations. In [5], a space-air-ground free-space optical (FSO) network incorporating a high-altitude relay was proposed to enhance the reliability of satellite communications. The works in [6]-[10] have focused on system-level optimization and design for dynamic satellite-terrestrial integrated networks, including network function placement, beam direction control, radio resource allocation, multicast transmission, and fog/edge computing architectures, with the objective of enhancing communication performance and quality of service. Recent studies, such as [11], have further explored advanced communication-computation co-design frameworks for integrated satellite and aerial networks. However, these studies mainly address system-level aspects rather than physical-layer performance analysis under practical impairments, such as co-channel interference. In [12]-[13], the authors evaluated secrecy performance of the HSTR

1. N. V. Toan is with Ho Chi Minh City University of Technology and Engineering, Ho Chi Minh City, Vietnam, and Telecommunications University, Nha Trang City, Vietnam. Email: toannv.ncs@hcmute.edu.vn
2. N. N. Lan, T. T. Duy (Corresponding Author) and N. T. Hieu are with Posts and Telecommunications Institute of Technology, Ha Noi, Vietnam. Emails: lannn@ptit.edu.vn, duytt@ptit.edu.vn and hieunt@ptit.edu.vn
3. P. N. Son is with Ho Chi Minh City Uni. of Technology and Engineering., Ho Chi Minh City, Vietnam Email: sonpndtvt@hcmute.edu.vn

schemes in the presence of eavesdroppers. In addition, Reference [12] examined a scenario involving multiple eavesdroppers, while Reference [13] proposed relay selection strategies. The authors of [14] investigated the trade-off between intercept probability (IP) at the eavesdropper and outage probability (OP) at legitimate receiver for the HSTR models. Furthermore, an effective relay selection mechanism was proposed in [14] to improve the IP/OP trade-off under the impact of co-channel interference (CCI). Researchers in [15]-[17] investigated the HSTR models operating in cognitive radio (CR) environments, where the licensed spectrum owned by primary users can be shared with secondary users, as long as operation of secondary users was not harmful to performance of primary users. Another research direction involves the use of wirelessly energy harvesting in the HSTR schemes [18]-[19]. Indeed, the wireless devices in [18]-[19] have to harvest energy from surrounding radio-frequency signals. In [20]-[21], full-duplex relay techniques have been investigated in the context of the HSTR schemes, enabling simultaneous data transmission and reception at relay nodes equipped with multiple antennas. Reference [22] introduced an HSTR scenario supported by reconfigurable intelligent surfaces (RIS). Unlike the conventional relaying approaches in which relay nodes actively process signals, RIS-based relaying models utilize intelligent reflective elements to direct incoming wireless signals toward intended destinations in an optimized manner. In [23]-[24], the authors integrated Non-Orthogonal Multiple Access (NOMA) into the HSTR systems, enabling the satellite to simultaneously transmit different data to multiple ground users. In [23], the authors proposed and derived expressions of OP for the NOMA -assisted HSTR systems. Reference [24] further considered the impact of direct communication links between the satellite and the ground NOMA users. The OP performance of the NOMA -based HSTR schemes operating in CR environments was evaluated in [25]. Reference [26] investigated both IP and OP performance for cognitive users in the NOMA -aided HSTR models. In [27], OP of multi-relay NOMA -based HSTR networks was also derived and validated. In contrast to the aforementioned studies, this paper considers the HSTR scheme that incorporates Fountain codes (FCs).

Fountain codes (FCs) [28]-[29] have demonstrated effectiveness in wireless networks, thanks to their ease of implementation and ability to adapt to changing environmental conditions. Recently, several studies [30]-[34] have reported on the HSTR models employing FCs. In [30], the OP performance of the HSTR model employing FCs under the CCI condition was evaluated. Reference [31] studied the OP/IP trade-off of the FCs -based HSTR schemes employing the artificial jamming technique to reduce quality of the eavesdropping links. In [32], both NOMA and RIS were integrated into the FC-aided HSTR systems to improve secrecy rate throughput, with the presence of multiple eavesdroppers. The authors of [33] investigated OP of joint NOMA and FC-based HSTR scenarios incorporating two groups of ground users. Published works [34] studied the OP/IP trade-off for the NOMA -aided HSTR multicast schemes using FCs and a partial terrestrial station selection algorithm.

To highlight the contribution of this work, Table 1 provides a comparative summary of representative FC-aided HSTR studies in terms of transmission scenario, interference modeling, performance metrics, and optimization capability.

Table 1. Summary and comparison of related works.

Ref.	Transmission Scenario	FC Used	CCI at Relay	CCI at Users	Performance Metrics	Time - Power Allocation
[30]	HSTR relaying (broadcast)	✓	*X*	✓	OP, SOP	*X*
[31]	STN with friendly jamming	✓	*X*	*X*	OP, IP	*X*
[32]	Multi-user HSTRN (NOMA + IRS)	✓	*X*	*X*	OP, IP	*X*
[33]	HSTR broadcast (NOMA-based)	✓	*X*	*X*	OP, SOP	*X*
[34]	HSTR multicast (NOMA + PRS)	✓	*X*	*X*	OP, IP, SOP, SIP	*X*
Our work	HSTR multicast with CCI	✓	✓	✓	OP, SOP	✓

As observed from Table 1, none of the existing studies jointly considers multicast transmission, dual CCI effects at both relay and users, and joint time-power allocation. More importantly, the interplay among these factors introduces several fundamental challenges beyond a straightforward combination of existing techniques.

Specifically, multicast transmission inherently couples the decoding performance of all users, making the system outage probability depending on the worst-channel condition, which significantly complicates the analysis compared to conventional unicast or broadcast scenarios. In addition, the presence of dual CCI at both the relay and user sides makes the end-to-end outage event jointly dependent on multiple transmission phases, thereby preventing the direct use of simplified independent-link analysis commonly adopted in prior studies. Furthermore, the joint optimization of time and power allocation under multicast and interference-limited conditions results in a highly coupled and non-convex problem, where the trade-off between reliability and interference mitigation becomes significantly more intricate. Therefore, the proposed framework should be regarded as a fundamentally new system model rather than a simple extension of existing works.

Motivated by these research gaps, this paper investigates FC-aided HSTR schemes, where a satellite communicates with a group of ground users *via* a terrestrial relay station. Unlike [31]-[34], our proposed schemes take into account the impact of CCI on the OP performance. In contrast to [30], this study considers the effect of CCI on both the relay station and all ground users. Furthermore, two FC-aided HSTR schemes are considered; namely, the conventional forwarding scheme (ConV) and the proposed packet-accumulation-based scheme (ProP), to address the identified research gaps. Compared with the ConV scheme, the proposed ProP scheme improves transmission reliability by exploiting the packet-accumulation property of FC. This design is particularly suitable for interference-limited or poor channel conditions, where packet-by-packet forwarding may become inefficient. For performance measurement, exact closed-form expressions of OP at each ground user and system outage probability (SOP) are derived for ConV and ProP. The accuracy of the analytical results is verified through computer simulations. Finally, a joint optimization problem involving time and power allocation is formulated and solved to enhance the SOP performance for the two considered schemes.

The main contributions of this paper can be summarized as follows:

- Development of an FC-aided HSTR multicast model under dual CCI affecting both relay and user nodes.
- Design of a packet-accumulation-based ProP scheme, in which the relay collects sufficient Fountain-coded packets before forwarding to improve transmission reliability.
- Derivation of exact closed-form expressions for the OP at each user and the SOP for both ConV and ProP schemes.
- Joint optimization of time and power allocation to minimize SOP using an efficient GSS-based approach.

The remainder of this article is organized as follows: Section 2 describes the system model of the proposed schemes. Section 3 derives OP and SOP of ConV and ProP. Section 4 provides Monte-Carlo simulations to validate the analytical formulae. Finally, Section 5 concludes the paper.

2. SYSTEM MODEL

Figure 1 presents the system model of the proposed FC-aided HSTRNs, with presence of K interference sources. In particular, a satellite (S) tries to send the same data w_{s} to M ground users. Let us denote the ground users as $\mathrm{U}_m(m = 1,2,\dots,M)$ and the interference sources as $\mathrm{I}_k(k = 1,2,\dots,K)$. It is assumed that there is no direct link between S and U_m, as we consider a worstcase scenario in which ground users experience blockage, severe shadowing, or significant path loss (e.g., urban canyon environments, indoor users, or obstructed areas), which are commonly encountered in practice and render the satellite-user link highly unreliable [13], [35]; therefore, the data transmission between S and U_m is assisted by a terrestrial relay station (R).

In the considered model, co-channel interference affects both decoding stages; namely the satellite-to-relay reception and the relay-to-user reception. Specifically, the relay is interfered by the links $\mathrm{I_k} \rightarrow \mathrm{R}$, while each user U_m is interfered by the links $\mathrm{I_k} \rightarrow \mathrm{U_m}$. We consider a normalized two-slot transmission framework with fixed slot duration and assume perfect synchronization between the satellite and the relay, which is consistently applied to both the ConV and ProP schemes.

Using FCs, S generates encoded packets (denoted as p_{S}) from the original data (w_{S}), and these encoded packets are then transmitted from S to U_m *via* the help of R , using the DF approach. In order to successfully recover the original data w_{S}, U_m needs to collect at least $G_{\min}$ encoded packets p_{S}, where

$G_{\min}$ represents the minimum number of packets required for FC decoding and is typically given by $G_{\min} = P(1+\varepsilon)$. Here, P denotes the number of source packets and ε is the small FC overhead that ensures reliable recovery (generally $\in [0.02,0.1]$) [29]-[31]. In addition, the satellite is allowed to transmit at most $N_{\max}$ encoded packets due to the delay constraints of the HSTR system. Since successful decoding is impossible if fewer than $G_{\min}$ packets are transmitted, the condition $N_{\max} \geq G_{\min}$ must always hold to guarantee recoverability at R and all ground users. These definitions help clarify the FC parameter selection used in the proposed multicast schemes. All nodes $\mathrm{S}, \mathrm{R}, \mathrm{U}_m$ and I_k are assumed to be equipped with a single antenna. This simplified model facilitates tractable analysis while still capturing the essential behavior of the considered system. Extensions to multiantenna scenarios will be investigated in future work.

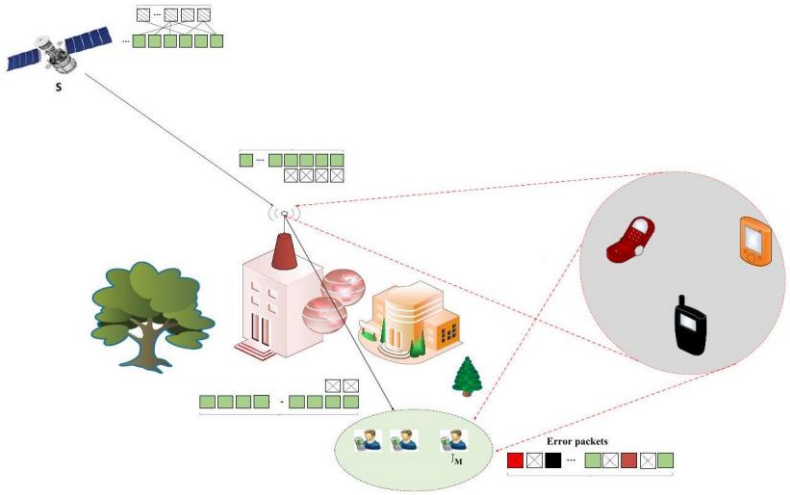

Figure 1. The proposed FC-aided HSTRs.

Let g_{AB} denote channel gain of the A → B channels, where A and B are a transmitter and a receiver, respectively, $(\mathrm{A},\mathrm{B}) \in \{\mathrm{S},\mathrm{R},\mathrm{U}_m,\mathrm{I}_k\}, m = 1,2,\ldots,M, k = 1,2,\ldots,K$. Assume that all A → B channels are block and flat fading, meaning that g_{AB} does not change during each transmission of p_{S}, but varies independently after each transmission of p_{S}.

For the S → R link, the channel gain g_{SR} which experiences a Shadowed-Rician distribution has the following PDF (see [30]-[31]):

$$f_{\gamma_{\mathrm{SR}}}(x) = \frac{1}{2b_{\mathrm{SR}}}\left(\frac{2a_{\mathrm{SR}}b_{\mathrm{SR}}}{2a_{\mathrm{SR}}b_{\mathrm{SR}}+\Omega_{\mathrm{SR}}}\right)^{a_{\mathrm{SR}}} \exp\left(-\frac{x}{2b_{\mathrm{SR}}}\right) {}_1F_1\left(a_{\mathrm{SR}};1;\frac{\Omega_{\mathrm{SR}}x}{2b_{\mathrm{SR}}(2a_{\mathrm{SR}}b_{\mathrm{SR}}+\Omega_{\mathrm{SR}})}\right), \quad (1)$$

where $2b_{\mathrm{SR}}$ and Ω_{SR} indicate the mean values of the multi-path and Line of Sight (LOS) components, respectively, a_{SR} is a fading parameter, and ${}_1F_1(.;.;.)$ is a confluent hypergeometric function of the first kind [30]-[31].

Using [34], CDF of g_{SR} can be expressed under the following form:

$$\begin{aligned} F_{\gamma_{\mathrm{SR}}}(x) &= 1 - \alpha_{\mathrm{SR}}^{a_{\mathrm{SR}}}\psi_{\mathrm{SR}} \sum_{n_{\mathrm{SR}}=0}^{a_{\mathrm{SR}}-1} \sum_{q_{\mathrm{SR}}=0}^{n_{\mathrm{SR}}} \frac{(n_{\mathrm{SR}})!}{(q_{\mathrm{SR}})!} \frac{\xi_{\mathrm{SR}}(n_{\mathrm{SR}})}{(\psi_{\mathrm{SR}}-\beta_{\mathrm{SR}})^{n_{\mathrm{SR}}-q_{\mathrm{SR}}+1}} x^{q_{\mathrm{SR}}} \exp(-(\psi_{\mathrm{SR}}-\beta_{\mathrm{SR}})x) \\ &= 1 - \sum_{n_{\mathrm{SR}}=0}^{a_{\mathrm{SR}}-1} \sum_{q_{\mathrm{SR}}=0}^{n_{\mathrm{SR}}} \Psi_0 x^{q_{\mathrm{SR}}} \exp(-(\psi_{\mathrm{SR}}-\beta_{\mathrm{SR}})x), \end{aligned} \quad (2)$$

where (n_{ST}) is Pochhammer function [34], and

$$\psi_{\mathrm{SR}} = \frac{1}{2b_{\mathrm{SR}}}, \alpha_{\mathrm{SR}} = \left(\frac{2a_{\mathrm{SR}}b_{\mathrm{SR}}}{2a_{\mathrm{SR}}b_{\mathrm{SR}}+\Omega_{\mathrm{SR}}}\right)^{a_{\mathrm{SR}}}, \beta_{\mathrm{SR}} = \left(\frac{\Omega_{\mathrm{SR}}}{2b_{\mathrm{SR}}(2a_{\mathrm{SR}}b_{\mathrm{SR}}+\Omega_{\mathrm{SR}})}\right),$$

$$\xi_{\mathrm{SR}}(n_{\mathrm{SR}}) = \frac{(-1)^{n_{\mathrm{SR}}}(1-a_{\mathrm{SR}})\beta_{\mathrm{SR}}^{n_{\mathrm{SR}}}}{(n_{\mathrm{SR}})!}, \Psi_0 = \frac{(n_{\mathrm{SR}})!}{(q_{\mathrm{SR}})!} \frac{\alpha_{\mathrm{SR}}^{a_{\mathrm{SR}}}\psi_{\mathrm{SR}}\xi_{\mathrm{SR}}(n_{\mathrm{SR}})}{(\psi_{\mathrm{SR}}-\beta_{\mathrm{SR}})^{n_{\mathrm{SR}}-q_{\mathrm{SR}}+1}}. \quad (3)$$

For the $\mathrm{R} \rightarrow \mathrm{U}_m, \mathrm{I}_k \rightarrow \mathrm{R}$ and $\mathrm{I}_k \rightarrow \mathrm{U}_m$ links, all these channels are assumed to be Rayleigh fading. Hence, $g_{\mathrm{RU}_m}, g_{\mathrm{I}_k\mathrm{R}}$ and $g_{\mathrm{I}_k\mathrm{U}_m}$ experience exponential distributions, and their PDFs can be written, respectively, as [36]:

$$f_{g_{\mathrm{RU}_m}}(x) = \lambda_{\mathrm{RU}_m}\exp\left(-\lambda_{\mathrm{RU}_m}x\right), f_{g_{\mathrm{t}\mathrm{R}_\mathrm{R}}}(x) = \lambda_{\mathrm{I}_k\mathrm{R}}\exp\left(-\lambda_{\mathrm{I}_k\mathrm{R}}x\right), f_{g_{\mathrm{I}_k\mathrm{U}_m}}(x) = \lambda_{\mathrm{I}_k\mathrm{U}_m}\exp\left(-\lambda_{\mathrm{I}_k\mathrm{U}_m}x\right), \quad (4)$$

where $\lambda_{\mathrm{RU}_m}, \lambda_{\mathrm{I}_k\mathrm{R}}$ and $\lambda_{\mathrm{I}_k\mathrm{R}_m}$ are fading parameters of the $\mathrm{R} \rightarrow \mathrm{U}_m, \mathrm{I}_k \rightarrow \mathrm{R}$ and $\mathrm{I}_k \rightarrow \mathrm{U}_m$ links, respectively [1].

As explained in [37], for ease of presentation and analytical tractability, the channel coefficients $g_{\mathrm{RU}_m}, g_{\mathrm{I}_k\mathrm{R}}$ and $g_{\mathrm{I}_k\mathrm{U}_m}$ can be assumed to be independent and identically distributed (i.i.d.). Similarly, all interference sources are assumed to have identical transmit power and experience i.i.d. Rayleigh fading, which enables the aggregate interference to be modelled in a tractable form [38]. Accordingly, the large-scale fading parameters satisfy $\lambda_{\mathrm{RU}_m} = \lambda_{\mathrm{RU}}(\forall m), \lambda_{\mathrm{I}_k\mathrm{R}} = \lambda_{\mathrm{IR}}(\forall k)$ and $\lambda_{\mathrm{I}_k\mathrm{U}_m} = \lambda_{\mathrm{IU}}(\forall k, m)$. This common assumption allows the decoding events to maintain a binomial structure and enables closed-form derivations in the subsequent analysis. Therefore, we can rewrite (4) under the following forms:

$$f_{g_{\mathrm{RU}_m}}(x) = \lambda_{\mathrm{RU}}\exp(-\lambda_{\mathrm{RU}}x), f_{g_{\mathrm{I}_\mathrm{R}\mathrm{R}}}(x) = \lambda_{\mathrm{IR}}\exp(-\lambda_{\mathrm{IR}}x), f_{g_{\mathrm{I}_k\mathrm{U}_m}}(x) = \lambda_{\mathrm{IU}}\exp(-\lambda_{\mathrm{IU}}x) \quad (5)$$

From (5), the corresponding CDFs can be obtained, respectively, as:

$$F_{g_{\mathrm{RU}_m}}(x) = 1 - \exp(-\lambda_{\mathrm{RU}}x), F_{g_{I_k\mathrm{R}}}(x) = 1 - \exp(-\lambda_{\mathrm{IR}}x), F_{g_{I_k\mathrm{U}_m}}(x) = 1 - \exp(-\lambda_{\mathrm{IU}}x) \quad (6)$$

Next, the operational principles of the conventional FC-aided HSTRNs (ConV) and the proposed FC-aided HSTRNs (ProP) are described in detail.

2.1 The ConV Scheme

In the ConV scheme, the relay station R forwards each encoded packet p_S to the ground users, without storing any p_S in its buffer. In particular, at the first time slot, S transmits p_S to R, and the instantaneous SNR obtained at R can be given as [39]:

$$\psi_{\mathrm{SR}}^{\mathrm{ConV}} = \frac{P_\mathrm{S} g_{\mathrm{SR}}}{\sum_{k=1}^{K} P_\mathrm{I} g_{\mathrm{I}_k\mathrm{R}} + \sigma_0^2} = \frac{\Delta_\mathrm{S} g_{\mathrm{SR}}}{\sum_{k=1}^{K} \Delta_\mathrm{I} g_{\mathrm{I}_k\mathrm{R}} + 1}, \quad (7)$$

where P_S and P_I are transmit power of the satellite S and all interference sources, respectively, σ_0^2 is variance of Gaussian noises at all receivers B, $\Delta_\mathrm{S} = P_\mathrm{S}/\sigma_0^2$ and $\Delta_\mathrm{I} = P_\mathrm{I}/\sigma_0^2$ denotes transmit SNRs.

If R decodes p_S successfully, it sends p_S to all the ground users at the second time slot, using the DF approach. The instantaneous SNR of the $\mathrm{R} \rightarrow \mathrm{U}_m$ link can be given as:

$$\psi_{\mathrm{RU}_m}^{\mathrm{ConV}} = \frac{P_\mathrm{R} g_{\mathrm{RU}_m}}{\sum_{k=1}^{K} P_\mathrm{I} g_{\mathrm{I}_k\mathrm{U}_m} + \sigma_0^2} = \frac{\Delta_\mathrm{R} g_{\mathrm{RU}_m}}{\sum_{k=1}^{K} \Delta_\mathrm{I} g_{\mathrm{I}_k\mathrm{U}_m} + 1}, \quad (8)$$

where P_R is transmit power of R , and $\Delta_\mathrm{R} = P_\mathrm{R}/\sigma_0^2$.

We now consider the time allocation between the first and second time slots in the ConV scheme. Assume that the total duration for the $\mathrm{S} \rightarrow \mathrm{R} \rightarrow \mathrm{U}$ transmission is 01-time unit. Let the time allocated to the first and second time slots be τ_{ConV} and $1 - \tau_{\mathrm{ConV}}$, respectively, where $0 < \tau_{\mathrm{ConV}} < 1$. Therefore, we can formulate the instantaneous channel capacity of the $\mathrm{S} \rightarrow \mathrm{R}$ and $\mathrm{R} \rightarrow \mathrm{U}_m$ links, respectively, as:

$$C_{\mathrm{SR}}^{\mathrm{ConV}} = \tau_{\mathrm{ConV}} \log_2\left(1 + \psi_{\mathrm{SR}}^{\mathrm{ConV}}\right),$$

$$C_{\mathrm{RU}_m}^{\mathrm{ConV}} = (1 - \tau_{\mathrm{ConV}}) \log_2\left(1 + \psi_{RU_m}^{ConV}\right) \quad (9)$$

2.2 The ProP Scheme

Similar to the ConV scheme, S sends p_S to R at the first time slot, and the instantaneous SNR obtained at R can be given, similarly, as (7):

$$\psi_{\mathrm{SR}}^{\mathrm{ProP}} = \frac{\Delta_\mathrm{S} g_{\mathrm{SR}}}{\sum_{k=1}^{K} \Delta_\mathrm{I} g_{\mathrm{I}_k\mathrm{R}} + 1}, \quad (10)$$

Let τ_{ProP} and $1-\tau_{\text{ProP}}$ denote the time allocated to the first and second time slots in the ProP scheme, where $0<\tau_{\text{ProP}}<1$. Then, the instantaneous channel capacity of the S → R link can be given as:

$$C_{\text{SR}}^{\text{PrOP}}=\tau_{\text{ProP}}\log_2\left(1+\psi_{\text{SR}}^{\text{PrOP}}\right) \tag{11}$$

If the decoding at R is successful, R sends p_{S} to all the ground users at the second time slot. Then, the instantaneous SNR of the R → U_m link can be given, similarly, as (8):

$$\psi_{\text{RU}_m}^{\text{ProP}^{\text{Pr}}}=\frac{\Delta_{\text{R}}g_{\text{RU}_m}}{\sum_{k=1}^{K}\Delta_{\text{I}}g_{\text{I}_k\text{U}_m}+1}. \tag{12}$$

Then, the instantaneous channel capacity of the R → U_m link can be expressed as:

$$C_{\text{RU}_m}^{\text{ProP,Case 1}}=(1-\tau_{\text{ProP}})\log_2\left(1+\psi_{\text{RU}_m}^{\text{ProP}}\right). \tag{13}$$

As mentioned, the relay station in ProP stores in its buffers the encoded packets which are correctly decoded. When the number of packets p_{S} correctly obtained at R equals $G_{\min}$, it can recover the original data. Moreover, R will replace S to transmit encoded packets to the ground users. After this point, the relay switches to the transmission phase and forwards encoded packets to the ground users. Due to the half-duplex constraint, the relay no longer attempts to receive additional packets from the satellite once it starts forwarding. Meanwhile, the satellite may continue transmitting up to $N_{\max}$, as limited by the system delay constraint. In addition, the packets transmitted by the relay are generated based on the recovered source data using Fountain coding, allowing the users to accumulate sufficient packets for successful decoding. In this case, the instantaneous channel capacity of the R → U_m link can be calculated as:

$$C_{\text{RU}_m}^{\text{ProP,Case 2}}=\log_2\left(1+\psi_{\text{RU}_m}^{\text{ProP}}\right) \tag{14}$$

Remark 1: The absence of a direct satellite-user link in the considered model represents a worst-case scenario commonly adopted in hybrid satellite-terrestrial networks. If a weak direct link is present, its contribution can be incorporated as an additional SINR component without altering the structure of the proposed ProP scheme. In this case, both OP and SOP are expected to improve due to additional diversity, while the relative performance gain of ProP over the conventional scheme remains intact.

3. PERFORMANCE ANALYSIS

This section derives exact closed-form expressions of OP and SOP for the ConV and ProP schemes. At first, we evaluate the decoding probability of one encoded packet p_{S}.

3.1 Decoding of the Packet p_{S}

It is worth noting that one packet p_{S} is successfully transmitted to U_m if both S → R and R → U_m transmissions are successful.

Indeed, considering the transmission of p_{S} at the first time slot in the ConV scheme; from (7) and (9), the probability of the correct decoding of p_{S} at R can be formulated as:

$$\begin{aligned}\theta_{\text{SR}}^{\text{ConV}}&=\Pr\left(C_{\text{SR}}^{\text{ConV}}\geq C_{1,\text{th}}\right)=\Pr\left(\psi_{\text{SR}}^{\text{ConV}}\geq\psi_{1,\text{th}}^{\text{ConV}}\right)=\Pr\left(g_{\text{SR}}\geq\frac{\Delta_{\text{I}}\psi_{1,\text{th}}^{\text{ConV}}}{\Delta_{\text{S}}}\sum_{k=1}^{K}g_{\text{I}_k\text{R}}+\frac{\psi_{1,\text{th}}^{\text{ConV}}}{\Delta_{\text{S}}}\right)\\&=\Pr\left(g_{\text{SR}}\geq\rho_{1,\text{th}}^{\text{ConV}}Z_{\text{R,Sum}}+\rho_{2,\text{th}}^{\text{ConV}}\right)\end{aligned} \tag{15}$$

where $C_{1,\text{ th}}$ is a target rate of the first link between S and R, $Z_{\text{R, Sum}}=\sum_{k=1}^{K}g_{\text{I}_k\text{R}}$, and

$$\psi_{1,\text{th}}^{\text{ConV}}=2^{\frac{C_{1,\text{th}}}{\tau_{\text{ConV}}}}-1,\rho_{1,\text{th}}^{\text{ConV}}=\frac{\Delta_{\text{I}}\psi_{1,\text{th}}^{\text{ConV}}}{\Delta_{\text{S}}},\rho_{2,\text{th}}^{\text{ConV}}=\frac{\psi_{1,\text{th}}^{\text{ConV}}}{\Delta_{\text{S}}} \tag{16}$$

Since $Z_{\text{R, Sum}}$ is a summation of K exponential random variables, using [40, eq. (B.9)], we obtain PDF of $Z_{\text{R,Sum}}$ as:

$$f_{Z_{\text{R, Sum}}}(x)=\frac{(\lambda_{\text{IR}})^K x^{K-1}\exp(-\lambda_{\text{IR}}x)}{(K-1)!} \tag{17}$$

Next, we can express $\theta_{\mathrm{SR}}^{\mathrm{ConV}}$ in (15) under the following form:

$$\theta_{\mathrm{SR}}^{\mathrm{ConV}} = \int_0^{+\infty} \left(1 - F_{g_{\mathrm{SR}}}\left(\rho_{1,\mathrm{th}}^{\mathrm{ConV}} x + \rho_{2,\mathrm{th}}^{\mathrm{ConV}}\right)\right) f_{Z_{\mathrm{R,Sum}}}(x) dx \tag{18}$$

From (2), we can express $F_{g_{\mathrm{SR}}}\left(\rho_{1,\mathrm{th}}^{\mathrm{ConV}} x + \rho_{2,\mathrm{th}}^{\mathrm{ConV}}\right)$ under the following form:

$$\begin{aligned} F_{\gamma_{\mathrm{SR}}}\left(\rho_{1,\mathrm{th}}^{\mathrm{ConV}} x + \rho_{2,\mathrm{th}}^{\mathrm{ConV}}\right) &= 1 - \sum_{n_{\mathrm{SR}}=0}^{a_{\mathrm{SR}}-1} \sum_{q_{\mathrm{SR}}=0}^{n_{\mathrm{SR}}} \Psi_1^{\mathrm{ConV}} \left(x + \rho_{3,\mathrm{th}}^{\mathrm{ConV}}\right)^{q_{\mathrm{SR}}} \exp\left(-\rho_{4,\mathrm{th}}^{\mathrm{ConV}} x\right) \\ &= 1 - \sum_{n_{\mathrm{SR}}=0}^{a_{\mathrm{SR}}-1} \sum_{q_{\mathrm{SR}}=0}^{n_{\mathrm{SR}}} \sum_{t_{\mathrm{SR}}=0}^{q_{\mathrm{SR}}} \Psi_1^{\mathrm{ConV}} \binom{q_{\mathrm{SR}}}{t_{\mathrm{SR}}} \left(\rho_{3,\mathrm{th}}^{\mathrm{ConV}}\right)^{t_{\mathrm{SR}}} x^{q_{\mathrm{SR}}-t_{\mathrm{SR}}} \exp\left(-\rho_{4,\mathrm{th}}^{\mathrm{ConV}} x\right) \\ &= 1 - \sum_{n_{\mathrm{SR}}=0}^{a_{\mathrm{SR}}-1} \sum_{q_{\mathrm{SR}}=0}^{n_{\mathrm{SR}}} \sum_{t_{\mathrm{SR}}=0}^{q_{\mathrm{SR}}} \Psi_2^{\mathrm{ConV}} x^{q_{\mathrm{SR}}-t_{\mathrm{SR}}} \exp\left(-\rho_{4,\mathrm{th}}^{\mathrm{ConV}} x\right), \end{aligned} \tag{19}$$

where

$$\rho_{3,\mathrm{th}}^{\mathrm{ConV}} = \frac{\rho_{2,\mathrm{th}}^{\mathrm{ConV}}}{\rho_{1,\mathrm{th}}^{\mathrm{ConV}}}, \rho_{4,\mathrm{th}}^{\mathrm{ConV}} = (\psi_{\mathrm{SR}} - \beta_{\mathrm{SR}}) \rho_{1,\mathrm{th}}^{\mathrm{ConV}}, \binom{q_{\mathrm{SR}}}{t_{\mathrm{SR}}} = \frac{(q_{\mathrm{SR}})!}{(t_{\mathrm{SR}})!\,(q_{\mathrm{SR}} - t_{\mathrm{SR}})!}$$

$$\Psi_1^{\mathrm{ConV}} = \Psi_0 \left(\rho_{1,\mathrm{th}}^{\mathrm{ConV}}\right)^{q_{\mathrm{SR}}} \exp\left(-(\psi_{\mathrm{SR}} - \beta_{\mathrm{SR}}) \rho_{2,\mathrm{th}}^{\mathrm{ConV}}\right), \Psi_2^{\mathrm{ConV}} = \binom{q_{\mathrm{SR}}}{t_{\mathrm{SR}}} \left(\rho_{3,\mathrm{th}}^{\mathrm{ConV}}\right)^{t_{\mathrm{SR}}} \Psi_1. \tag{20}$$

Substituting (17) and (19) into (18), after some manipulations, we obtain an exact closed-form expression of $\theta_{\mathrm{SR}}^{\mathrm{ConV}}$ as:

$$\begin{aligned} \theta_{\mathrm{SR}}^{\mathrm{ConV}} &= \sum_{n_{\mathrm{SR}}=0}^{a_{\mathrm{SR}}-1} \sum_{q_{\mathrm{SR}}=0}^{n_{\mathrm{SR}}} \sum_{t_{\mathrm{SR}}=0}^{q_{\mathrm{SR}}} \frac{(\lambda_{\mathrm{IR}})^K \Psi_2}{(K-1)!} \int_0^{+\infty} x^{K+q_{\mathrm{SR}}-t_{\mathrm{SR}}-1} \exp\left(-\left(\rho_{4,\mathrm{th}}^{\mathrm{ConV}} + \lambda_{\mathrm{IR}}\right) x\right) dx \\ &= \sum_{n_{\mathrm{SR}}=0}^{a_{\mathrm{SR}}-1} \sum_{q_{\mathrm{SR}}=0}^{n_{\mathrm{SR}}} \sum_{t_{\mathrm{SR}}=0}^{q_{\mathrm{SR}}} \frac{(K + q_{\mathrm{SR}} - t_{\mathrm{SR}} - 1)!}{(K-1)!} \frac{(\lambda_{\mathrm{IR}})^K \Psi_2^{\mathrm{ConV}}}{\left(\lambda_{\mathrm{IR}} + \rho_{4,\mathrm{th}}^{\mathrm{ConV}}\right)^{K+q_{\mathrm{SR}}-t_{\mathrm{SR}}}} \end{aligned} \tag{21}$$

Considering the transmission at the second time slot in the ConV scheme; the probability of the successful decoding of one encoded packet p_{S} at U_m can be formulated by using (8) and (9) as:

$$\begin{aligned} \theta_{\mathrm{RU}_m}^{\mathrm{ConV}} = \Pr\left(C_{\mathrm{RU}_m}^{\mathrm{ConV}} \geq C_{2,\mathrm{th}}\right) &= \Pr\left(\psi_{\mathrm{RU}_m}^{\mathrm{ConV}} \geq \psi_{2,\mathrm{th}}^{\mathrm{ConV}}\right) = \Pr\left(g_{\mathrm{RU}_m} \geq \frac{\Delta_{\mathrm{I}} \psi_{2,\mathrm{th}}^{\mathrm{ConV}}}{\Delta_{\mathrm{R}}} \sum_{k=1}^{K} g_{\mathrm{I}_k \mathrm{U}_m} + \frac{\psi_{2,\mathrm{th}}^{\mathrm{ConV}}}{\Delta_{\mathrm{R}}}\right) \\ &= \Pr\left(g_{\mathrm{RU}_m} \geq \omega_{1,\mathrm{th}}^{\mathrm{ConV}} Z_{\mathrm{U}_m,\mathrm{Sum}} + \omega_{2,\mathrm{th}}^{\mathrm{ConV}}\right) \end{aligned} \tag{22}$$

where $C_{2,\mathrm{th}}$ is a target rate of the $\mathrm{R} \to \mathrm{U}_m$ link, $Z_{\mathrm{U}_m,\mathrm{Sum}} = \sum_{k=1}^{K} g_{\mathrm{I}_k \mathrm{U}_m}$, and

$$\psi_{2,\mathrm{th}}^{\mathrm{ConV}} = 2^{\frac{C_{2,\mathrm{th}}}{1-\tau_{\mathrm{ConV}}}} - 1, \omega_{1,\mathrm{th}}^{\mathrm{ConV}} = \frac{\Delta_{\mathrm{I}} \psi_{2,\mathrm{th}}^{\mathrm{ConV}}}{\Delta_{\mathrm{R}}}, \omega_{2,\mathrm{th}}^{\mathrm{ConV}} = \frac{\psi_{2,\mathrm{th}}^{\mathrm{ConV}}}{\Delta_{\mathrm{R}}}. \tag{23}$$

Similar to (17), PDF of $Z_{\mathrm{U}_m,\,\mathrm{Sum}}$ can be expressed as:

$$f_{Z_{\mathrm{U}_m,\,\mathrm{Sum}}}(x) = \frac{(\lambda_{\mathrm{IU}})^M x^{M-1} \exp(-\lambda_{\mathrm{IU}} x)}{(M-1)!} \tag{24}$$

Substituting (6) and (24) into (22), after some manipulations, we obtain an exact closed-form expression of $\theta_{\mathrm{RU}_m}^{\mathrm{ConV}}$ as:

$$\begin{aligned} \theta_{\mathrm{RU}_m}^{\mathrm{ConV}} &= \int_0^{+\infty} \left[1 - F_{g_{\mathrm{RU}_m}}\left(\omega_{1,\mathrm{th}}^{\mathrm{ConV}} x + \omega_{2,\mathrm{th}}^{\mathrm{ConV}}\right)\right] f_{Z_{\mathrm{U}_m,\mathrm{Sum}}}(x) dx \\ &= \frac{(\lambda_{\mathrm{IU}})^M}{(M-1)!} \exp\left(-\lambda_{\mathrm{RU}} \omega_{2,\mathrm{th}}^{\mathrm{ConV}}\right) \int_0^{+\infty} x^{M-1} \exp\left(-\left(\lambda_{\mathrm{IU}} + \lambda_{\mathrm{RU}} \omega_{1,\mathrm{th}}^{\mathrm{ConV}}\right) x\right) dx \\ &= \left(\frac{\lambda_{\mathrm{IU}}}{\lambda_{\mathrm{IU}} + \lambda_{\mathrm{RU}} \omega_{1,\mathrm{th}}^{\mathrm{ConV}}}\right)^M \exp\left(-\lambda_{RU} \omega_{2,th}^{ConV}\right) \end{aligned} \tag{25}$$

Then, the probability of the successful decoding of one packet p_S at U_m in the ConV scheme is computed as:

$$\theta_{U_m}^{\text{ConV}} = \theta_{\text{SR}}^{\text{ConV}} \theta_{\text{RU}_m}^{\text{ConV}} \tag{26}$$

Considering the ProP scheme; the probability that one packet p_S is decoded correctly by the user U_m can be calculated in two cases as follows: Case 1: p_S is sent to U_m via the S → R → U_m link; Case 2: p_S is directly transmitted from R to U_m.

Case 1: p_S is sent to U_m *via* the S → R → U_m link

Similar to (21) and (24), the probability that one packet p_S is decoded correctly at the S → R and R → U_m links can be given, respectively, as:

$$\theta_{\text{SR}}^{\text{ProP}} = \sum_{n_{\text{SR}}=0}^{a_{\text{SR}}-1} \sum_{q_{\text{SR}}=0}^{n_{\text{SR}}} \sum_{t_{\text{SR}}=0}^{q_{\text{SR}}} \frac{(K+q_{\text{SR}}-t_{\text{SR}}-1)!}{(K-1)!} \frac{(\lambda_{\text{IR}})^K \Psi_2^{\text{ProP}}}{\left(\lambda_{\text{IR}}+\rho_{4,\text{th}}^{\text{ProP}}\right)^{K+q_{\text{SR}}-t_{\text{SR}}}}, \tag{27}$$

$$\theta_{\text{RU}}^{\text{ProP, Case 1}} = \left(\frac{\lambda_{\text{IU}}}{\lambda_{\text{IU}}+\lambda_{\text{RU}}\omega_{1,\text{th}}^{\text{ProP}}}\right)^M \exp\left(-\lambda_{\text{RU}}\omega_{2,\text{th}}^{\text{ProP}}\right), \tag{28}$$

where

$$\psi_{1,\text{th}}^{\text{ProP}} = 2^{\frac{C_{1,\text{th}}}{\tau_{\text{ProP}}}} - 1, \rho_{1,\text{th}}^{\text{ProP}} = \frac{\Delta_{\text{I}}\psi_{1,\text{th}}^{\text{ProP}}}{\Delta_{\text{S}}}, \rho_{2,\text{th}}^{\text{ProP}} = \frac{\psi_{1,\text{th}}^{\text{ProP}}}{\Delta_{\text{S}}}, \rho_{3,\text{th}}^{\text{ProP}} = \frac{\rho_{2,\text{th}}^{\text{ProP}}}{\rho_{1,\text{th}}^{\text{ProP}}}, \rho_{4,\text{th}}^{\text{ProP}} = (\psi_{\text{SR}} - \beta_{\text{SR}})\rho_{1,\text{th}}^{\text{ProP}},$$

$$\Psi_1^{\text{ProP}} = \Psi_0\left(\rho_{1,\text{th}}^{\text{ProP}}\right)^{q_{\text{SR}}} \exp\left(-(\psi_{\text{SR}} - \beta_{\text{SR}})\rho_{2,\text{th}}^{\text{ProP}}\right), \Psi_2^{\text{ProP}} = \binom{q_{\text{SR}}}{t_{\text{SR}}} \left(\rho_{3,\text{th}}^{\text{ProP}}\right)^{t_{\text{SR}}} \Psi_1^{\text{ProP}},$$

$$\psi_{2,\text{th}}^{\text{ProP}} = 2^{\frac{C_{2,\text{th}}}{1-\tau_{\text{ConV}}}} - 1, \omega_{1,\text{th}}^{\text{ProP}} = \frac{\Delta_{\text{I}}\psi_{2,\text{th}}^{\text{ProP}}}{\Delta_{\text{R}}}, \omega_{2,\text{th}}^{\text{ProP}} = \frac{\psi_{2,\text{th}}^{\text{ProP}}}{\Delta_{\text{R}}}, \tag{29}$$

Case 2: p_S is directly transmitted from R to U_m

In this case, using (14) instead of (13) for Case 2, we can obtain the probability that p_S is successfully transmitted from R to U_m as

$$\theta_{\text{RU}_m}^{\text{ProP,Case2}} = \left(\frac{\lambda_{\text{IU}}}{\lambda_{\text{IU}}+\lambda_{\text{RU}}\omega_{3,\text{th}}^{\text{ProP}}}\right)^M \exp\left(-\lambda_{\text{RU}}\omega_{4,\text{th}}^{\text{ProP}}\right), \tag{30}$$

where

$$\psi_{3,\text{th}}^{\text{PrOP}} = 2^{C_{2,\text{th}}} - 1, \omega_{3,\text{th}}^{\text{ProP}} = \frac{\Delta_{\text{I}}\psi_{3,\text{th}}^{\text{ProP}}}{\Delta_{\text{R}}}, \omega_{4,\text{th}}^{\text{PrOP}} = \frac{\psi_{3,\text{th}}^{\text{ProP}}}{\Delta_{\text{R}}} \tag{31}$$

3.2 Outage Probability (OP) at Each User

Considering the ConV scheme; let denote L_m^{ConV} as the number of p_S that is correctly received at U_m. If $L_m^{\text{ConV}} < G_{\min}$, U_m cannot reconstruct the original data of the satellite. Hence, OP at U_m in ConV can be expressed by an exact closed-form expression as:

$$\begin{aligned}\text{OP}_m^{\text{ConV}} &= 1 - \sum_{T_S=G_{\min}}^{N_{\max}} \Pr\left(L_R^{\text{ConV}} = G_{\min}, T_S\right) \Pr\left(L_m^{\text{ConV}} \geq G_{\min} \mid T_S\right) \\ &= \sum_{L_m^{\text{ConV}}=0}^{G_{\min}-1} \binom{N_{\max}}{L_m^{\text{ConV}}} \left(\theta_{U_m}^{\text{ConV}}\right)^{L_m^{\text{ConV}}} \left(1-\theta_{U_m}^{\text{ConV}}\right)^{N_{\max}-L_m^{\text{ConV}}}\end{aligned} \tag{32}$$

where $\left(1-\theta_{U_m}^{\text{ConV}}\right)$ is the probability that p_S cannot be successfully reached to U_m. For the ProP scheme; we consider the probability that the user U_m can successfully recover the original data of the satellite. Indeed, if we denote L_m^{ProP} as the number of p_S that is correctly received at U_m, then $L_m^{\text{ProP}} \geq G_{\min}$. It is worth noting that if L_R^{ProP} denotes the number of p_S being correctly received at R, then L_R^{ProP} must be equal to $G_{\min}$. It is because if $L_R^{\text{ProP}} < G_{\min}$, then $L_m^{\text{ProP}} < L_R^{\text{ProP}} < G_{\min}$, and U_m is

then in outage. Then, let us denote T_{S} as the number of transmission times of the satellite until the station R collects enough $G_{\min}$ encoded packets p_{S}, where $G_{\min} \le T_{\mathrm{S}} \le N_{\max}$. Therefore, the number of transmission times of R in Case 2 is given as $T_{\mathrm{R}} = N_{\max} - T_{\mathrm{S}}$. We also denote $L_{m,\,\mathrm{Casel}}^{\mathrm{ProP}}$ as the number of p_{S} that is correctly received at U_m in Case 1, where $0 \le L_{m,\,\mathrm{Casel}}^{\mathrm{ProP}} \le T_{\mathrm{S}}$. Finally, the successful reconstruction of the original data at U_m in ProP can be formulated as:

$$\overline{\mathrm{OP}}_m^{\mathrm{ProP}} = 1 - \sum_{T_{\mathrm{S}}=G_{\min}}^{N_{\max}} \Pr\left(L_R^{\mathrm{ProP}} = G_{\min}, T_{\mathrm{S}}\right) \Pr\left(L_{m,\,\mathrm{Case1}}^{\mathrm{ProP}} + L_{m,\,\mathrm{Case\,2}}^{\mathrm{ProP}} \ge G_{\min} \mid T_{\mathrm{S}}\right). \quad (33)$$

In (33), $\Pr\left(L_{\mathrm{R}}^{\mathrm{ProP}} = G_{\min}, T_{\mathrm{S}}\right) = \binom{T_{\mathrm{S}}-1}{G_{\min}-1} \left(\theta_{\mathrm{SR}}^{\mathrm{ProP}}\right)^{G_{\min}} \left(1-\theta_{\mathrm{SR}}^{\mathrm{ProP}}\right)^{T_{\mathrm{S}}-G_{\min}}$ is the probability that R collects enough $G_{\min}$ encoded packets p_{S} after T_{S} transmission times of S. It is worth noting that the transmission between S and R at the T_{S}-th transmission must be successful, and R must correctly receive $G_{\min} - 1$ packets p_{S} previously.

$\binom{G_{\min}}{L_{m,\,\mathrm{Case\,1}}^{\mathrm{ProP}}} \left(\theta_{\mathrm{RU}_m}^{\mathrm{ProP,Case\,1}}\right)^{L_{m,\,\mathrm{Casel}}^{\mathrm{Prop}}} \left(1-\theta_{\mathrm{RU}_m}^{\mathrm{ProP,Case\,1}}\right)^{G_{\min}-L_{m,\,\mathrm{Casel}}^{\mathrm{ProP}}}$ is the probability that U_m correctly receives $L_{m,\,\mathrm{Casel}}^{\mathrm{ProP}}$ packets p_{S} in Case 1, and $\mathrm{OP}_m^{\mathrm{ProP}} \binom{N_{\max}-T_{\mathrm{S}}}{L_{m,\,\mathrm{Case1}}^{\mathrm{ProP}}} \left(\theta_{\mathrm{RU}_m}^{\mathrm{ProP,Case\,2}}\right)^{L_{m,\,\mathrm{Case2}}^{\mathrm{ProP}}} \left(1-\theta_{\mathrm{RU}_m}^{\mathrm{ProP,Case\,2}}\right)^{N_{\max}-T_{\mathrm{S}}-L_{m,\,\mathrm{Case\,2}}^{\mathrm{Prop}}}$ is the probability that U_m correctly receives $L_{m,\,\mathrm{Case2}}^{\mathrm{ProP}}$ packets p_{S} in Case 2. Then, OP at U_m in ProP is obtained as:

$$\mathrm{OP}_m^{\mathrm{ProP}} = 1 - \overline{\mathrm{OP}}_m^{\mathrm{ProP}} \quad (34)$$

Remark 2: Since the R → U and I → U links are independent and identical, it is straightforward that OP at all the users in the considered schemes is the same, i.e., we can write $\mathrm{OP}_m^{\mathrm{ConV}} = \mathrm{OP}^{\mathrm{ConV}}$ and $\mathrm{OP}_m^{\mathrm{ProP}} = \mathrm{OP}^{\mathrm{ProP}}$ for $\forall m$.

3.3 System Outage Probability (SOP)

Firstly, $\mathrm{SOP}_{\mathrm{X}}$ is defined as the probability that one of the users in the X scheme experiences an outage, where $\mathrm{X} \in \{\mathrm{ConV}, \mathrm{ProP}\}$. To obtain $\mathrm{SOP}_{\mathrm{X}}$, we have to consider the probability that all the users can successfully recover the original data of the satellite, i.e., $\overline{\mathrm{SOP}_{\mathrm{X}}} = 1 - \mathrm{SOP}_{\mathrm{X}}$.

Considering the ConV scheme; let us denote $L_{\mathrm{R}}^{\mathrm{ConV}}$ as the number of p_{S} that is correctly received by the station R after the transmission ends. In order that all the users can collect at least $G_{\min}$ packets p_{S}, we have $G_{\min} \le L_{\mathrm{R}}^{\mathrm{ConV}} \le N_{\max}$. Then, $\overline{\mathrm{SOP}}_{\mathrm{ConV}}$ can be computed as:

$$\begin{aligned}\overline{\mathrm{SOP}}_{\mathrm{ConV}} &= 1 - \sum_{L_{\mathrm{R}}^{\mathrm{ConV}}=G_{\min}}^{N_{\max}} \Pr\left(L_{\mathrm{R}}^{\mathrm{ConV}} = L_R\right) \Pr\left(L_m^{\mathrm{ConV}} \ge G_{\min}, \forall m \mid L_{\mathrm{R}}^{\mathrm{ConV}} = L_R\right) \\ &= \sum_{L_{\mathrm{R}}^{\mathrm{ConV}}=G_{\min}}^{N_{\max}} \left\{ \begin{array}{l} \binom{N_{\max}}{L_{\mathrm{R}}^{\mathrm{ConV}}} \left(\theta_{\mathrm{SR}}^{\mathrm{ConV}}\right)^{L_{\mathrm{R}}^{\mathrm{ConV}}} \left(1-\theta_{\mathrm{SR}}^{\mathrm{ConV}}\right)^{N_{\max}-L_{\mathrm{R}}^{\mathrm{ConV}}} \\ \times \prod_{m=1}^{M} \left[\sum_{L_m^{\mathrm{ConV}}=G_{\min}}^{L_{\mathrm{R}}^{\mathrm{ConV}}} \binom{L_m^{\mathrm{ConV}}}{L_{\mathrm{R}}^{\mathrm{ConV}}} \left(\theta_{\mathrm{RU}}^{\mathrm{ConV}}\right)^{L_m^{\mathrm{ConV}}} \left(1-\theta_{\mathrm{RU}}^{\mathrm{ConV}}\right)^{L_{\mathrm{R}}^{\mathrm{ConV}}-L_m^{\mathrm{ConV}}} \right] \end{array} \right\} \end{aligned} \quad (35)$$

In (35), $\Pr\left(L_m^{\mathrm{ConV}} \ge G_{\min}, \forall m \mid L_{\mathrm{R}}^{\mathrm{ConV}} = L_R\right) = \sum_{L_m^{\mathrm{ConV}}=G_{\min}}^{L_{\mathrm{R}}^{\mathrm{ConV}}} \binom{L_m^{\mathrm{ConV}}}{L_{\mathrm{R}}^{\mathrm{ConV}}} \left(\theta_{\mathrm{RU}_m}^{\mathrm{ConV}}\right)^{L_m^{\mathrm{ConV}}} \left(1-\theta_{\mathrm{RU}_m}^{\mathrm{ConV}}\right)^{L_{\mathrm{R}}^{\mathrm{ConV}}} - L_m^{\mathrm{ConV}}$ is the probability that U_m can successfully receive at least $G_{\min}$ encoded packets.

Considering the ProP scheme; using (33), we can obtain $\overline{\mathrm{SOP}}_{\mathrm{ProP}}$ as:

$$\overline{\mathrm{SOP}}_{\mathrm{ProP}} = 1 - \sum_{T_{\mathrm{S}}=G_{\min}}^{N_{\max}} \Pr\left(L_{\mathrm{R}}^{\mathrm{ProP}} = G_{\min}, T_S\right) \prod_{m=1}^{M} \Pr\left(L_{m,\,\mathrm{Case1}}^{\mathrm{ProP}} + L_{m,\,\mathrm{Case\,2}}^{\mathrm{ProP}} \ge G_{\min}, \forall m \mid T_S\right) \quad (36)$$

Finally, SOP of the ConV and ProP schemes can be obtained, respectively, as:

$$\mathrm{SOP}_{\mathrm{ConV}} = 1 - \overline{\mathrm{SOP}}_{\mathrm{ConV}}, \mathrm{SOP}_{\mathrm{ProP}} = 1 - \overline{\mathrm{SOP}}_{\mathrm{ProP}}. \quad (37)$$

Remark 3: It is worth emphasizing that the proposed FC-assisted HSTR framework fundamentally differs from non-FC schemes. While non-FC approaches typically define OP/SOP based on instantaneous SINR constraints at the symbol level, the FC-assisted scheme evaluates OP/SOP through packet-level decoding conditions governed by $G_{\min}$ and $N_{\max}$. This packet accumulation mechanism allows successful decoding as long as a sufficient number of packets is collected, thereby offering improved robustness against channel fading and co-channel interference.

3.4 Joint Time and Power Allocation Problem

Assume that the total transmit power of the S and R nodes is fixed such that $P_S + P_R = P_{tot}$. Specifically, we examine the following power-allocation scheme: $P_S = \mu_x P_{tot}, P_R = (1 - \mu_x)P_{tot}$, where $X \in \{ConV, ProP\}$ and $0 < \mu_X < 1$. Now, we consider the joint time and power allocation problem as

$$\mathrm{Min}_{0<\tau_x<1, 0<\mu_x<1} \mathrm{SOP}_X. \quad (38)$$

Regarding the convergence of the adopted Golden-Section Search (GSS) algorithm, it is well known that GSS is guaranteed to converge for any continuous unimodal (or quasi-unimodal) function over a compact interval. In our optimization problem, the SOP-based objective function in (38) is continuous with respect to μ_X and τ_X on the bounded domain (0,1), which satisfies the classical convergence conditions of GSS [41]. In addition, we have numerically verified in all simulation settings that the iterative values μ_X^n and τ_X^n converge monotonically toward their optimal solutions within a small number of iterations (typically fewer than 20). This numerical behavior is fully consistent with the theoretical contraction factor $\varphi^{-1} \approx 0.618$ of GSS.

Moreover, the number of iterations is mainly determined by the stopping tolerance δ (commonly, $\delta = 10^{-4}: 10^{-3}$ is selected), and the GSS procedure is not sensitive to the choice of initial values, since the search is performed over predefined feasible intervals. Therefore, a convergence figure is not required, and the algorithm's convergence is theoretically ensured and empirically confirmed [42]. It is worth noting that the proposed optimization operates over low-dimensional variables and does not scale combinatorially with the number of users. The computational complexity of the GSS-based method is logarithmic with respect to the desired accuracy, which ensures efficient convergence. Therefore, the proposed approach remains computationally efficient and practically feasible even in large-scale user scenarios.

4. RESULTS

This section presents Monte-Carlo simulations (Sim) to verify the exact closed-form expressions (Theory) of OP and SOP for the ConV and ProP schemes. The simulation parameters are selected based on commonly adopted settings in the literature [12], [14], [31], [34]. Unless otherwise stated, the simulation parameters are set as follows: the Shadowed-Rician parameters $(a_{SR}, b_{SR}, \Omega_{SR})$ are (1,0.063,0.0007) or FHS and (5,0.251,0.279) for AS; the target rates are $C_{1,\mathrm{th}} = 0.2$, and $C_{2,\mathrm{th}} = 0.1$ and the average channel gains are $\lambda_{RU} = 1, \lambda_{IR} = 50$ and $\lambda_{IU} = 25$. In addition, $K = 3, G_{\min} = 6, \sigma_0^2 = 1$, and $P_I = 0.25P_{tot}$, while the transmit SNR is defined as $\Delta = P_{tot}/\sigma_0^2$. In Figure 2, we additionally include one example under the FHS condition with $N_{\max} = 8$ to illustrate the performance degradation caused by severe shadowing. For the remaining figures (Figs. 3-8), we present results only under the AS channel, since both AS and FHS exhibit the same OP and SOP variation trends, and including all FHS cases would not provide further analytical insight. Prior studies, such as [21], [23], have also confirmed that FHS yields consistently worse performance than AS due to harsher propagation conditions.

In Figure 2, we present OP at each user in the ConV and ProP schemes as a function of transmit SNR($\Delta = P_{tot}/\sigma_0^2$) in dB when $\mu_{ConV} = \mu_{ProP} = 0.5$ and $\tau_{ConV} = \tau_{ProP} = 0.5$. At first, it is remined that OP at each user in the two considered schemes is the same. Next, we can observe that the OP performance of both ConV and ProP is better as Δ increases, since transmit power of the satellite and the relay station increases. However, as $\Delta \to +\infty$, it can be seen that OP of both ConV and ProP reaches saturation values. It is because at high Δ regions, SINRs of the S → R and R → U_m links do not depend on Δ. Indeed, with $P_S = \mu P_{tot}, P_R = (1 - \mu)P_{tot}$ and $P_I = 0.25P_{tot}$, SINRs in (7), (8), (10) and (12) at high Δ can be approximated as follows:

$$\psi_{\mathrm{SR}}^{\mathrm{X}} \overset{\Delta\to+\infty}{\approx} \frac{\mu_{\mathrm{X}} g_{\mathrm{SR}}}{\sum_{k=1}^{K} 0.25 g_{\mathrm{I}_k\mathrm{R}} + 1}, \psi_{\mathrm{RU}_m}^{\mathrm{X}} \overset{\Delta\to+\infty}{\approx} \frac{(1-\mu_{\mathrm{X}}) g_{\mathrm{RU}_m}}{\sum_{k=1}^{K} 0.25 g_{\mathrm{I}_k\mathrm{U}_m} + 1}, \quad (39)$$

where $\mathrm{X} \in \{\mathrm{Con}V, ProP\}$.

Next, we can observe from Figure 2 that the OP performance of ConV and ProP is better as increasing $N_{\max}$. It is due to the fact that with higher $N_{\max}$, the ground users have more opportunity to sufficiently collect encoded packets for the data recovery. It is worth noting from Figure 2 that when $N_{\max} = 6$, the performance of ConV and ProP is the same, because in this case $N_{\max} = G_{\min}$. On the other hand, when $N_{\max} = 7$ and 8, the ProP scheme outperforms the ConV scheme. Furthermore, for the FHS condition with $N_{\max} = 8$, the OP variation of both schemes follows the same trend as in the AS case; however, due to the harsher propagation environment, the OP values under FHS are noticeably higher. It is also seen that as increasing $N_{\max}$, the performance gap between ConV and ProP also increases. It is noted that the effect of the Fountain coding overhead ε can be equivalently interpreted through $G_{\min} = (1 + \varepsilon)P$. For a fixed $G_{\min}$, increasing $N_{\max}$ relaxes the decoding constraint, leading to a reduction in OP [28], [34]. This reveals a trade-off between coding overhead and transmission constraint in Fountain-coded systems. Finally, Figure 2 presents that the 'Sim' results validate the 'Theory' ones.

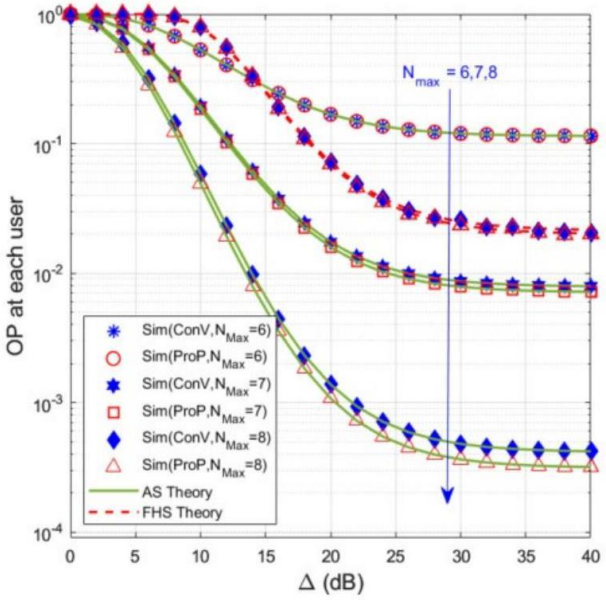

Figure 2. OP at each user as a function of Δ(dB) when $\mu_{\mathrm{ConV}} = \mu_{\mathrm{ProP}} = 0.5$ and $\tau_{\mathrm{ConV}} = \tau_{\mathrm{ProP}} = 0.5$.

Figure 3 presents OP at each user in ConV and ProP as a function of τ_{ConV} and τ_{ProP} when $\Delta = 20$ dB and $N_{\max} = 8$. As we can see from Figure 3, $\tau_{\mathrm{X}}(\mathrm{X} \in \{\mathrm{ConV}, \mathrm{ProP}\})$ significantly impacts the OP performance. Moreover, for each value of μ_{X}, there exists an optimal value of τ_{X} at which OP at each user in the X scheme is lowest. For example, with $\mu_{\mathrm{ConV}} = \mu_{\mathrm{ProP}} = 0.9$, OP at each user in ConV and ProP is minimized at $\tau_{\mathrm{ConV}} = 0.3$ and $\tau_{\mathrm{ProP}} = 0.35$, respectively. Figure 3 also illustrates that the OP performance of both ConV and ProP is almost best as $\mu_{\mathrm{ConV}} = \mu_{\mathrm{ProP}} = 0.5$. This is because when μ_{ConV} and μ_{ProP} are very low ($\mu_{\mathrm{ConV}} = \mu_{\mathrm{ProP}} = 0.1$), the transmit power of the satellite (S) is also very low. Conversely, when μ_{ConV} and μ_{ProP} are very high ($\mu_{\mathrm{ConV}} = \mu_{\mathrm{ProP}} = 0.9$), the transmit power of the relay station (R) becomes very low. These conditions result in a high OP at each user. Finally, Figure 3 again shows that ProP outperforms ConV, and the 'Sim' and 'Theory' results match very well.

In Figure 4, we present SOP of the ConV and ProP schemes as a function of Δ(dB) when $\mu_{\mathrm{ConV}} = \mu_{\mathrm{ProP}} = 0.5, \tau_{\mathrm{ConV}} = \tau_{\mathrm{ProP}} = 0.5$, and $N_{\max} = 8$. Similar to the OP at each user, the SOP values decrease as Δ increases, and converge to the saturation values at high Δ regimes. It is also seen that the SOP of ProP is lower that that of ConV. Moreover, the SOP performance of ConV and ProP is worse with higher number of ground users (M). Finally, it is worth noting that the 'Sim' results validate the 'Theory' ones.

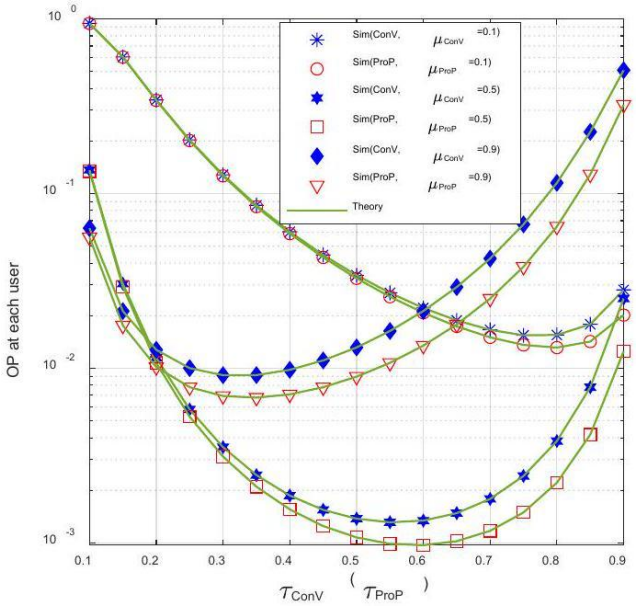

Figure 3. OP at each user as a function of τ_{ConV} (τ_{ProP}) when $\Delta = 20$ dB and $N_{\max} = 8$.

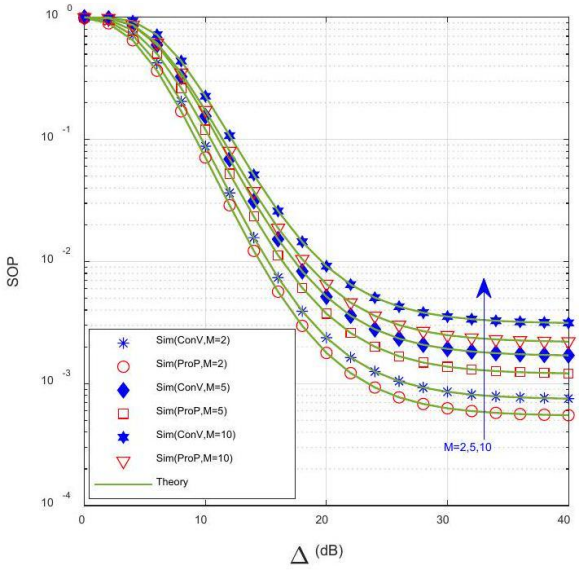

Figure 4. SOP as a function of Δ(dB) when $\mu_{\mathrm{ConV}} = \mu_{\mathrm{ProP}} = 0.5, \tau_{\mathrm{ConV}} = \tau_{\mathrm{ProP}} = 0.5$, and $N_{\max} = 8$.

Figure 5 presents SOP of the ConV and ProP schemes as a function of τ_{ConV} (τ_{ProP}) when $\Delta = 20(\text{ dB}), \mu_{\mathrm{ConV}} = \mu_{\mathrm{ProP}} = 0.65,$ and $M = 5$. We can see that the SOP performance of both ConV and ProP is significantly better when $N_{\max}$ increases from 7 to 8 . It is also observed that there exist optimal values of τ_{ConV} (τ_{ProP}) so that SOP of ConV (ProP) is lowest. For example, with $N_{\max} = 7$, SOP of ConV and ProP is lowest at $\tau_{\mathrm{ConV}} = 0.4$ and $\tau_{\mathrm{ProP}} = 0.45$, respectively. In addition, with $N_{\max} = 8$, SOP of ConV and ProP is lowest at $\tau_{\mathrm{ConV}} = 0.45$ and $\tau_{\mathrm{ProP}} = 0.5$, respectively. Similarly, the impact of ε on SOP is reflected through $G_{\min}$. A larger $G_{\min}$ requires more successfully received packets, whereas a larger $N_{\max}$ increases the decoding opportunity and hence reduces SOP.

Figure 6 investigates the impact of μ_{ConV} (μ_{ProP}) on the SOP performance of ConV and ProP with $\Delta = 15(\text{ dB}), M = 8,$ and $N_{\max} = 9$. As observed, there exist optimal values of μ_{ConV} and μ_{ProP}, so that SOP of ConV and ProP is lowest. For ConV, we can observe that SOP is lowest when $\tau_{\mathrm{ConV}} = 0.55$ and $\mu_{\mathrm{ConV}} = 0.5$, while ProP obtains the best performance when $\tau_{\mathrm{ProP}} = 0.55$ and $\mu_{\mathrm{ProP}} = 0.55$.

From Figures 5 and 6, it is worth noting that the joint time and power allocation problem (see (42)) must be solved to determine the optimal values of the ($\tau_{\mathrm{x}}, \mu_{\mathrm{x}}$) pairs, where $\mathrm{X} \in \{\mathrm{ConV}, \mathrm{ProP}\}$. To achieve this, the Golden-section search algorithm presented in [42] can be employed.

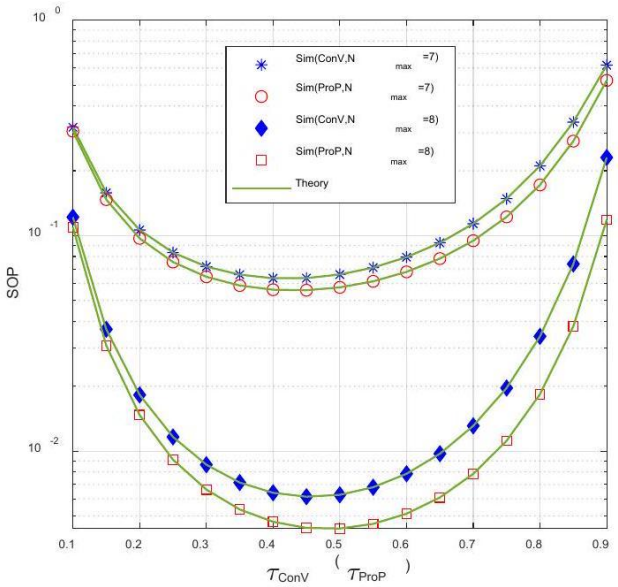

Figure 5. SOP as a function of τ_{ConV} (τ_{ProP}) when $\Delta = 20(\text{ dB})$, $\mu_{\text{ConV}} = \mu_{\text{ProP}} = 0.65$, and $M = 5$.

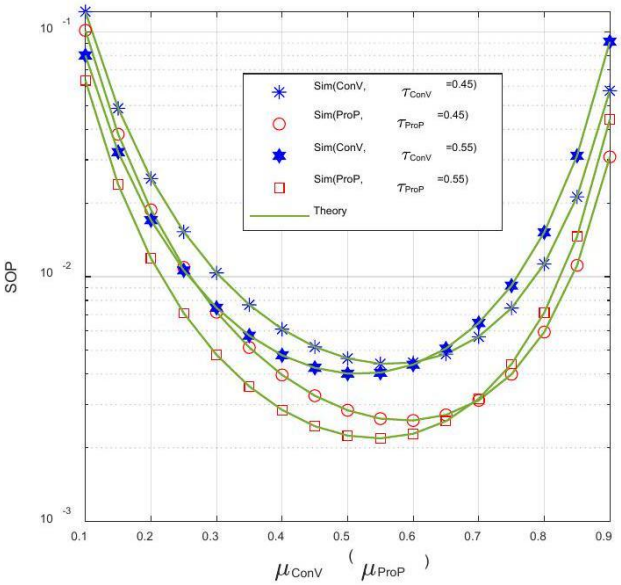

Figure 6. SOP as a function of μ_{ConV} (μ_{ProP}) when $\Delta = 15(\text{ dB}), M = 8$, and $N_{\max} = 9$.

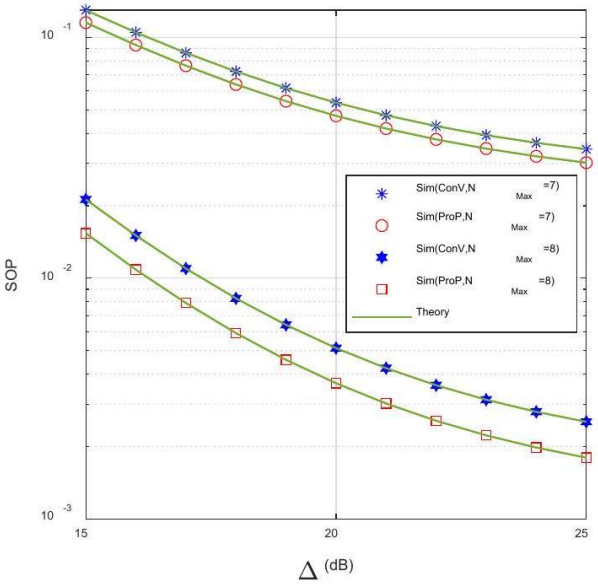

Figure 7. SOP as a function of $\Delta(\text{dB})$ with optimal values of ($\mu_{\text{X}}, \tau_{\text{X}}$) when $M = 5$.

Table 2. Optimal values of ($\mu_{\mathrm{X}}, \tau_{\mathrm{X}}$) in Figure 7 when $N_{\max} = 7$.

Δ	15 dB	16 dB	17 dB	18 dB	19 dB	20 dB	21 dB	22 dB	23 dB	24 dB	25 dB
μ^*_{ConV}	0.485	0.482	0.479	0.476	0.474	0.471	0.469	0.467	0.465	0.464	0.462
τ^*_{ConV}	0.501	0.499	0.496	0.494	0.491	0.489	0.487	0.485	0.483	0.482	0.481
μ^*_{ProP}	0.488	0.485	0.482	0.479	0.477	0.474	0.472	0.470	0.468	0.466	0.464
τ^*_{ProP}	0.512	0.510	0.507	0.504	0.502	0.499	0.497	0.495	0.494	0.492	0.491

Figure 7 presents SOP as a function of Δ in dB with various values of $N_{\max}$ and with $M = 5$. In this figure, the ($\mu_{\mathrm{X}}, \tau_{\mathrm{X}}$) pair is optimized according to equation (38). Indeed, Tables 2 and 3 present the optimal values of ($\mu_{\mathrm{X}}, \tau_{\mathrm{X}}$) in the case where $N_{\max} = 7$ and $N_{\max} = 8$, respectively. For example, in Table 2, with $N_{\max} = 7$ and $\Delta = 20$ dB, SOP of the ConV and ProP schemes is lowest at $(\mu_{\mathrm{ConV}}, \tau_{\mathrm{ConV}}) = (0.471, 0.489)$ and $(\mu_{\mathrm{ProP}}, \tau_{\mathrm{ProP}}) = (0.477, 0.502)$. For another example, in Table 3, with $N_{\max} = 8$ and $\Delta = 20$ dB, the optimal values of $(\mu_{\mathrm{X}}, \tau_{\mathrm{X}})$ are given as follows: $(\mu_{\mathrm{ConV}}, \tau_{\mathrm{ConV}}) = (0.503, 0.518)$ and $(\mu_{\mathrm{ProP}}, \tau_{\mathrm{ProP}}) = (0.509, 0.540)$. As seen from Figure 7, SOP of both ConV and ProP significantly decreases as increasing $N_{\max}$ and Δ. In addition, the performance gap between ConV and ProP also increases as $N_{\max}$ increases from 7 to 8.

Table 3. Optimal values of ($\mu_{\mathrm{X}}, \tau_{\mathrm{X}}$) in Figure 7 when $N_{\max} = 8$.

Δ	15 dB	16 dB	17 dB	17 dB	19 dB	20 dB	21 dB	22 dB	23 dB	24 dB	25 dB
μ^*_{ConV}	0.515	0.513	0.510	0.508	0.505	0.503	0.501	0.498	0.497	0.495	0.494
τ^*_{ConV}	0.529	0.527	0.525	0.522	0.520	0.518	0.516	0.514	0.512	0.511	0.509
μ^*_{ProP}	0.522	0.520	0.517	0.514	0.512	0.509	0.507	0.504	0.502	0.501	0.499
τ^*_{ProP}	0.551	0.549	0.547	0.544	0.542	0.540	0.537	0.536	0.534	0.533	0.531

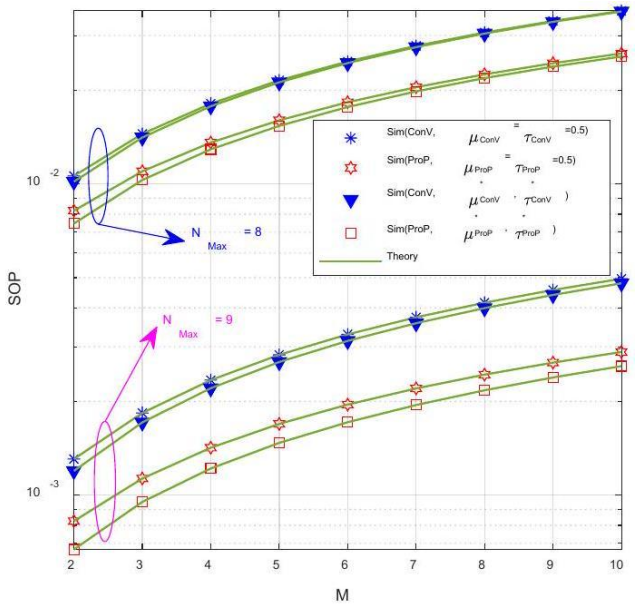

Figure 8. SOP as a function of M when $\Delta = 15$(dB).

Figure 8 presents the SOP performance of the considered schemes as a function of the number of ground users (M) with $\Delta = 15$(dB) and with two cases: i) the optimal values of ($\mu_{\mathrm{X}}, \tau_{\mathrm{X}}$); and $(\mu_{\mathrm{X}}, \tau_{\mathrm{X}}) = (0.5, 0.5)$. To simplify the presentation, the optimal values of the ($\mu_{\mathrm{X}}, \tau_{\mathrm{X}}$) pairs in Figure 8 will not be presented. As seen from Figure 8, SOP of both ConV and ProP increases as M increases. It is due to the fact that with higher number of ground users, the probability that at least one user experiences an outage, resulting in a higher SOP. Again, we can see that the SOP performance can be significantly enhanced by increasing $N_{\max} = 8$. In addition, ProP outperforms ConV, and the performance gap between ConV and ProP increases as increasing $N_{\max}$.

5. CONCLUSIONS

In this paper, we derived exact closed-form expressions of OP and SOP for both ConV and ProP schemes. These expressions were validated through Monte-Carlo simulations. Based on the derived SOP, we conducted the joint time and power allocation. The results demonstrate that the proposed scheme (ProP) outperforms the conventional scheme (ConV), in terms of both OP and SOP. Moreover, the performance gap in SOP between the two schemes increases as the number of transmission times ($N_{\max}$) increases. The findings also indicate that the SOP performance of ConV and ProP can be further improved by optimizing the time and power allocation parameters and by increasing $N_{\max}$. However, it is important to note that increasing $N_{\max}$ also leads to higher delay time and power consumption.

ACKNOWLEDGEMENTS

This work is supported by Posts and Telecommunications Institute of Technology in 2026.

REFERENCES

[1] S. Chen, S. Sun and S. Kang, "System Integration of Terrestrial Mobile Communication and Satellite Communication: Trends, Challenges and Key Technologies in B5G and 6G," China Communications, vol. 17, no. 12, pp. 156-171, 2020.

[2] E. Cianca et al., "Integrated Satellite-HAP systems", IEEE Communications Magazine, vol. 43, no. 12, pp. supl.33-supl.39, 2005.

[3] K. An and T. Liang, "Hybrid Satellite-terrestrial Relay Networks with Adaptive Transmission", IEEE Transactions on Vehicular Technology, vol. 68, no. 12, pp. 12448-12452, 2019.

[4] X. Li, W. Feng, J. Wang, Y. Chen, N. Ge and C. -X. Wang, "Enabling 5G on the Ocean: A Hybrid Satellite-UAV-terrestrial Network Solution," IEEE Wireless Comm., vol. 27, no. 6, pp. 116121, 2020.

[5] K. Mashiko et al., "Combined Control of Coverage Area and HAPS Deployment in Hybrid FSO/RF SAGIN," IEEE Transactions on Vehicular Technology, vol. 74, no. 7, pp. 10819-10828, 2025.

[6] S. Yuan, Y. Sun and M. Peng, "Joint Network Function Placement and Routing Optimization in Dynamic Software-defined Satellite-terrestrial Integrated Networks," IEEE Transactions on Wireless Communications, vol. 23, no. 5, pp. 5172-5186, DOI: 10.1109/TWC.2023.3324729, May 2024.

[7] S. Yuan, Y. Sun, M. Peng and R. Yuan, "Joint Beam Direction Control and Radio Resource Allocation in Dynamic Multi-Beam LEO Satellite Networks," IEEE Transactions on Vehicular Technology, vol. 73, no. 6, pp. 8222-8237, DOI: 10.1109/TVT.2024.3353339, June 2024.

[8] S. Yuan, Y. Sun and M. Peng, "Cache-aware Cooperative Multicast Beamforming in Dynamic Satellite-terrestrial Networks," IEEE Transactions on Vehicular Technology, vol. 74, no. 1, pp. 1433-1445, 2025.

[9] S. Yuan, M. Peng and Y. Sun, "Satellite-terrestrial Integrated Fog Networks: Architecture, Technologies, and Challenges," IEEE Wireless Communications, vol. 32, no. 4, pp. 208-215, August 2025.

[10] C. Ding, J. -B. Wang, H. Zhang, M. Lin and G. Y. Li, "Joint MIMO Precoding and Computation Resource Allocation for Dual-function Radar and Communication Systems with Mobile Edge Computing," IEEE Journal on Selected Areas in Communications, vol. 40, no. 7, pp. 2085-2102, July 2022.

[11] B. Zhao, M. Lin, B. Ma, J. Ouyang, N. Al-Dhahir and M. -S. Alouini, "LDM-based Communication and Computation Co-design in Integrated Satellite and Aerial Networks," IEEE Transactions on Communications, vol. 73, no. 11, pp. 10230-10245, DOI: 10.1109/TCOMM.2025.3568218, Nov. 2025.

[12] Q. Huang et al., "Secrecy Performance of Hybrid Satellite-Terrestrial Relay Networks in the Presence of Multiple Eavesdroppers," IET Communications, vol. 12, no. 1, pp. 26-34, 2018.

[13] W. Cao, Y. Zou, Z. Yang and J. Zhu, "Relay Selection for Improving Physical-layer Security in Hybrid Satellite-terrestrial Relay Networks," IEEE Access, vol. 6, pp. 65275-65285, 2018.

[14] W. Cao et al., "Security-reliability Trade-off Analysis of Hybrid Satellite-terrestrial Uplink Communications with Relay Selection," IEEE Systems Journal, vol. 18, no. 1, pp. 485-496, 2024.

[15] K. Guo, K. An, B. Zhang, Y. Huang and G. Zheng, "Outage Analysis of Cognitive Hybrid Satellite-terrestrial Networks with Hardware Impairments and Multi-primary Users," IEEE Wireless Communications Letters, vol. 7, no. 5, pp. 816-819, 2018.

[16] V. Singh, S. Solanki and P. K. Upadhyay, "Cognitive Relaying Cooperation in Satellite-terrestrial Systems with Multiuser Diversity," IEEE Access, vol. 6, pp. 65539-65547, 2018.

[17] Y. Guo, M. Lin, Y. Liu, H. Kong, J. -B. Wang and J. Wang, "AoI-aware Uplink CR-NOMA Schemes in Satellite Internet of Things Networks," IEEE Transactions on Aerospace and Electronic Systems, vol. 61, no. 1, pp. 1224-1230, DOI: 10.1109/TAES.2024.3451455, Feb. 2025.

[18] V. Singh, P. K. Upadhyay, D. B. da Costa and U. S. Dias, "Hybrid Satellite-terrestrial Spectrum Sharing Systems with RF Energy Harvesting," Proc. of 2018 IEEE 29th Annual Int. Symposium on Personal, Indoor and Mobile Radio Communications (PIMRC), pp. 306-311, Bologna, Italy, 2018.

[19] Z. Li, G. Wang and M. Yang, "Performance Analysis of SWIPT Aided Satellite-terrestrial Cooperative Network," Proc. of the 2nd Asia-Pacific Conf. on Communications Technology and Computer Science (ACCTCS), pp. 252-256, Shenyang, China, 2022.

[20] V. Singh and P. K. Upadhyay, "Exploiting FD/HD Cooperative-NOMA in Underlay Cognitive Hybrid Satellite-terrestrial Networks," IEEE Transactions on Cognitive Communications and Networking, vol. 8, no. 1, pp. 246-262, 2022.

[21] T. N. Nguyen et al., "Outage Performance of Satellite Terrestrial Full-duplex Relaying Networks with Co-channel Interference," IEEE Wireless Communications Letters, vol. 11, no. 7, pp. 1478-1482, 2022.

[22] Z. Lin et al., "Refracting RIS-aided Hybrid Satellite-terrestrial Relay Networks: Joint Beamforming Design and Optimization," IEEE Transactions on Aerospace and Electronic Systems, vol. 58, no. 4, pp. 3717-3724, 2022.

[23] X. Yan, H. Xiao, C.-X. Wang and K. An, "Outage Performance of NOMA-based Hybrid Satellite-terrestrial Relay Networks", IEEE Wireless Communications Letters, vol. 7, no. 4, pp. 538-541, 2018.

[24] L. Han, W.-P. Zhu and M. Lin, "Outage of NOMA-based Hybrid Satellite-terrestrial Multi-antenna DF Relay Networks," IEEE Wireless Communications Letters, vol. 10, no. 5, pp. 1083-1087, 2021.

[25] V. Singh, V. Bankey and P. K. Upadhyay, "Underlay Cognitive Hybrid Satellite-terrestrial Networks with Cooperative-NOMA," Proc. of 2020 IEEE Wireless Communications and Networking Conf. (WCNC), pp. 1-6, Seoul, Korea, 2020.

[26] H. -N. Nguyen et al., "Reliable and Secure Transmission in Multiple Antennas Hybrid Satellite-terrestrial Cognitive Networks Relying on NOMA," IEEE Access, vol. 8, pp. 215044-215056, 2020.

[27] L. Han, W.-P. Zhu and M. Lin, "Outage Analysis of Multi-relay NOMA-based Hybrid Satellite-terrestrial Relay Networks," IEEE Transactions on Vehicular Technology, vol. 71, no. 6, pp. 64696487, 2022.

[28] D. J. C. MacKay, "Fountain Codes," IEE Proceedings-Communications, vol. 152, no. 6, pp. 10621068, 2005.

[29] T. L. Thanh et al., "Broadcasting in Cognitive Radio Networks: A Fountain Codes Approach," IEEE Transactions on Vehicular Technology, vol. 71, no. 10, pp. 11289-11294, 2022.

[30] N. V. Toan et al., "Outage Performance of Hybrid Satellite-terrestrial Relaying Networks with Rateless Codes in Co-channel Interference Environment," Proc. of 2023 Int. Conf. on System Science and Engineering (ICSSE), pp. 468-473, Ho Chi Minh, Vietnam, 2023.

[31] N. Q. Sang, et al., "On the Security and Reliability Trade-off of the Satellite Terrestrial Networks with Fountain Codes and Friendly Jamming," EAI Endorsed Transactions on Industrial Networks and Intelligent Systems, vol. 10, no. 4, e3, 2023.

[32] P. M. Quang et al., "Performance Enhancement for Rateless Codes-aided Hybrid Satellite-terrestrial Multi-user Networks Using NOMA and IRS with Presence of Multiple Eavesdroppers," Proc. of the 9th Int. Conf. on Consumer Electronics Asia (ICCE-Asia), pp. 1-4, Danang, Vietnam, 2024.

[33] N. V. Toan et al., "Performance Evaluation of Hybrid Satellite-terrestrial Relaying Broadcast Networks Using Fountain Codes and NOMA," Proc. of 2024 IEEE Int. Conf. on Consumer Electronics-Asia (ICCE-Asia), pp. 1-4, Danang, Vietnam, 2024.

[34] N. V. Toan, T. T. Duy, P. N. Son, P. V. Tuan and L. T. Tu, "Security-reliability Analysis of NOMA-assisted Hybrid Satellite-terrestrial Relay Multi-cast Transmission Networks Using Fountain Codes and Partial Relay Selection with Presence of Multiple Eavesdroppers," EAI Transactions on Industrial Networks and Intelligent Systems, vol. 12, no. 03, pp. 1-11, 2025.

[35] L. Han, W.-P. Zhu, and M. Lin, "Uplink outage performance of NOMA-based hybrid satellite-terrestrial relay networks over generalized inhomogeneous fading channels," IEEE Transactions on Communications, vol. 70, no. 4, pp. 2417-2434, 2022.

[36] N. Q. Sang et al., "Securing Wireless Communications with Energy Harvesting and Multi-antenna Diversity", Jordanian Journal of Computers and Information Technology (JJCIT), vol. 11, no. 02, pp. 197-210, June 2025.

[37] D.-H. Ha, T. T. Duy, P. N. Son, T. Le-Tien and M. Voznak, "Security-reliability Trade-off Analysis for Rateless Codes-based Relaying Protocols Using NOMA, Cooperative Jamming and Partial Relay Selection," IEEE Access, vol. 9, pp. 131087-131108, 2021.

[38] T. N. Nguyen et al., "Outage Performance of Satellite Terrestrial Full-duplex Relaying Networks with Co-channel Interference," IEEE Wireless Communications Letters, vol. 11, no. 7, pp. 1478-1482, 2022.

[39] N. Q. Sang et al., " Power Beacon-assisted Energy Harvesting in D2D Network under Co-channel Interferences: Symbol Error Rate Analysis ", Jordanian Journal of Computers and Information Technology (JJCIT), vol. 11, no. 04, pp. 517-532, December 2025.

[40] A.-T. Le et al., "Physical Layer Security Analysis for RIS-aided NOMA Systems with Non-colluding Eavesdroppers," Computer Communications, vol. 219, pp. 194-203, 2024.

[41] B. Li, Y. Zou, T. Wu, Z. Zhang, M. Chen and Y. Jiang, "Security and Reliability Tradeoff of NOMA Based Hybrid Satellite-terrestrial Network with a Friendly Jammer," IEEE Transactions on Vehicular Technology, vol. 74, no. 2, pp. 3439-3444, Feb. 2025.

[42] E. K. P. Chong and S. H. Zak, An Introduction to Optimization, DOI: 10.1002/9781118033340, ISBN: 9780471758006, United States: Wiley, 2008.

ملخص البحث:

نـدرس فـي هـذه الورقـة أداء الانقطـاع لأنظمـة البـث المتعـدّد الهجينـة عبـر الأقمـار الصّـناعية والشّـبكات الأرضـية باسـتخدام رمـوز (Fountain). فـي المخطّطـات المدروسـة، يحـاول القمـر الصّـناعي إرسـال بياناتـه إلـى مجموعـة مـن المسـتخدمين الأرضـيّين بمسـاعدة محطّـة تقويـة أرضـية. فـي المخطـط التّقليـدي (ConV)، تقـوم محطّـة التّقويـة بإعـادة توجيـه كـل حزمـة بيانـات (Fountain) إلـى المسـتخدمين الأرضيّين باستخدام تقنية فكّ التّشفير وإعادة التّوجيه.

أمّـا فـي المخطّـط المقتـرح (PropP)، فتقـوم محطّـة التّقويـة بتخـزين حـزم بيانـات (Fountain) المسـتلمة مـن القمـر الصّـناعي، وتقـوم مقـام القمـر الصّـناعي فـي إرسـال حـزم بيانـات (Fountain) جديـدة إلـى المسـتخدمين الأرضـيّين بمجـرّد جمّـع عـددٍ كـافٍ مـن حـزم بيانـات (Fountain) لاسـتعادة البيانـات. ونسـتنج صِـيغاً مغلقـة دقيقـة لاحتماليـة انقطـاع الطّاقـة عنـد كـل مسـتخدم، ولحتماليـة انقطـاع الخدمـة للمخطّطـين المـذكورين (التّقليدي والمقترح) مع مراعاة تأثير التّداخل بين القنوات المتجاورة.

وقـد تـمّ إجـراء محاكـاة حاسـوبية للتّحقُّـق مـن صـحّة الصِّـيغ المسـتخدمة. عـلاوةً علـى ذلـك، تمّـت صـياغة مسـألة مشـتركة وحلّهـا لتخصـيص الوقـت والطّاقـة معـاً لتحسـين أداء احتمالية لنقطاع الخدمة للنّظام في المخطّطين المدروسين.

This article is an open access article distributed under the terms and conditions of the Creative Commons Attribution (CC BY) license (http://creativecommons.org/licenses/by/4.0/).